Journal of Applied Electrochemistry **33**: 403–410, 2003.
© 2003 *Kluwer Academic Publishers. Printed in the Netherlands.*

Anisotropic copper etching with monoethanolamine-complexed cupric ion solutions

C-W. SHIH, Y-Y. WANG and C-C. WAN*
Department of Chemical Engineering, Tsing-Hua University, Hsin-Chu, Taiwan
*(*author for correspondence, e-mail: ccwan@che.nthu.edu.tw)*

Received 8 July 2002; accepted in revised form 4 February 2003

Key words: etching factor, inhibition, monoethanolamine, non-ammonia etching

Abstract

Monoethanolamine (MEA)-complexed cupric ion solution was used as a non-ammoniacal solution for copper etching on printed circuit boards (PCB). The copper dissolution behaviour of this MEA-complexed cupric solution containing 1 M $CuCl_2$ and 3.3 to 10 M MEA was studied by the potentiodynamic method at various temperatures (25–55 °C) and pH values (10–6.5). The effects of these factors on dissolution rate and etching factor of the copper patterns of PCBs were discussed. It was found that the highest corrosion current density (i_{corr}) was obtained with MEA concentration at about 5 M. Activation energies (E_a) of MEA-complexed cupric solutions were measured and the heat of adsorption (ΔH_{ads}), which accounts for the chemisorption of the MEA ligands on the copper surface was calculated. ΔH_{ads} was found to increase with solution containing excess MEA ([MEA] > 5 M), indicating the inhibition behaviour of MEA. Hence with lower pH, i_{corr} increased because the concentration of MEA ligands decreased due to acid reaction. The etching factor of copper patterns of PCBs with 75 μm/75 μm, line/space (L/S), were also tested by spray etching method. A high etching factor can be achieved for etchants containing high MEA concentration, which means MEA affects the etching factor since the inhibitive property of MEA reduces the undercut. Although the etching rate of MEA-complexed cupric etchant is still much lower than the ammoniacal etchant, the etching factor of the forward etchant (>3) is better than the latter (<2).

1. Introduction

Copper etching is an important process in manufacturing printed circuit boards (PCBs) and other circuitry-formation applications. Ammoniacal cupric etchant is one of the most commonly used because of its high etching rate (40–70 μm min^{-1}) and high capacity for dissolved copper (>170 g l^{-1}) [1]. However, there are important performance criteria other than etching rate and capacity. As etching proceeds vertically, the side-walls tend to be etched sideways and produce an undercut action. The degree to which this occurs is known as the etching factor (f) [2], which is defined as the ratio of depth to side attack and is commonly calculated using

$$f = \frac{2H}{b-a} \tag{1}$$

where H is the copper line thickness, a and b are the top and bottom width of copper line after etching, respectively. A high etching factor means relatively minor undercut for an etching process. In practice, controlled spray etching tends to lead to a high etching factor and immersion etching generally results in a low etching factor [3–5].

Although most studies have focused on the copper dissolution rate [6–9], the profile of copper lines after etching has recently received increasing attention [3, 10–14]. High-density circuitry on outer layers of PCBs specially requires anisotropic etching for fine-line formation. Serious undercut of copper etching by ammoniacal cupric etchant leads to low etching factor (~2) for copper fine lines ($\leqslant$3 mil). Inhibitors like benzotriazole (BTA), pyrazole and 5-nitro-1H indazole, have been all tried as 'banking agent' for copper etching but the results have been less than satisfactory [15–17]. In addition, the toxic nature of ammoniacal etchant also induces need for substitution [18].

Several non-fuming chelating agents including tartaric acid, malic acid, glycollic acid, ethylenediaminotetraacetic (EDTA), monoethanolamine (MEA, $H_2NCH_2CH_2$-OH) and their derivatives have been proposed to replace ammonia in preparing copper etchant [19]. Those etchants become are less toxic and can operate under neutral pH conditions, which is more compatible with many resists.

Tseng et al. [6] found MEA-complexed cupric solution to be most promising to as a non-ammoniacal etchant, since it tends to reduce undercut although its etching rate is still much lower than the ammoniacal etchant [1, 2].

Trivich [20] studied cupric ion complexed with MEA by polarography. The complex was found to contain four MEA ligands, as shown in Equation 2,

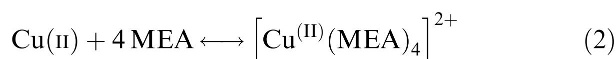

$$\mathrm{Cu(II)} + 4\,\mathrm{MEA} \longleftrightarrow \left[\mathrm{Cu^{(II)}(MEA)_4}\right]^{2+} \tag{2}$$

and the formation constant (K_f) of this complex ion is 3×10^{16}. MEA can function as a cupric chelate agent as well as inhibitor on copper [21, 22]. So MEA may serve well both as an etchant component and as an effective banking agent.

El-Sayed et al. [23] have studied copper dissolution in copper complex medium, but detail quantitative information is still insufficient. In this laboratory, we have studied the kinetics of copper dissolution with MEA-complexed cupric ion solution and found that adding bridging ligands like NaCl, NaBr, NaI or NaSCN can accelerate copper dissolution in MEA-complexed solution. The accelerating effect can be explained in terms of electron transfer via the inner-sphere mechanism [24]. However the operating conditions for a practical process needs further exploration, which constitutes the major focus of this research.

In the present study, the kinetic behaviour of copper etching in MEA-complexed cupric solution is investigated. From a theoretical point of view, the etching rate and etching factor of an etchant must be related to the chemistry of cupric ion and the associated ligands. Therefore, the objective of this study is to conduct a basic study on the reaction between cupric ions and MEA complex.

2. Experimental details

2.1. *Preparation of solutions*

MEA-complexed cupric solution was prepared with cupric chloride dihydrate ($CuCl_2.2\ H_2O$, Shown), reagent-grade monoethanolamine ($H_2NCH_2CH_2OH$, MEA, Tedia 99.9%) and deionized water. The concentration of cupric ion and MEA ligand was kept at 1 M and 3.3 to 10 M, respectively. A commercial ammoniacal etchant (main constituents are $CuCl_2$, NH_4OH, NH_4Cl plus banking agents, pH 8.5) was used for comparison. The initial pH value of all solutions was adjusted with sulfuric acid and sodium hydroxide. Absorption spectra of various etchants were recorded with an HP 8453 u.v.–vis. photodiode array spectrophotometer equipped with a 1 cm path length quartz cell. The concentration of Cu(II) present in the form of $Cu(MEA)_4^{2+}$ was determined by atomic absorption spectroscopy (Perkin Elmer Instrument Analyst 300).

2.2. *Electrochemical measurements*

Potentiodynamic experiments were carried out in solutions containing different MEA concentrations and at various temperatures (25–55 °C) and pH values (10–6.5). The copper dissolution rate was measured with a Solartron SI 1286 electrochemical interface potentio/galvanostat. The corrWare corrosion analysis software was used to control the potentio/galvanostat and record the data. The working electrode was a rotating copper disc insulated in Teflon. The area of copper disc exposed to the solution was 1.15 cm^2. The counter electrode was a platinum plate and a saturated calomel electrode (SCE) with a luggin capillary was used as the reference. The rotation speed was controlled at 1000 rpm. The corrosion potential (E_{corr}) was obtained by measuring the open-circuit potential (o.c.p.) which reached steady state after 2 h [25]. Corrosion current density (i_{corr}) was obtained by using the Tafel extrapolation method. Measurements were first performed with potential ranging ±200 mV from the corrosion potential at a sweep rate of 0.5 mV s^{-1}. The corrosion current density was then calculated from the Tafel line. The i_{corr} value at different reaction times was determined with each solution, respectively.

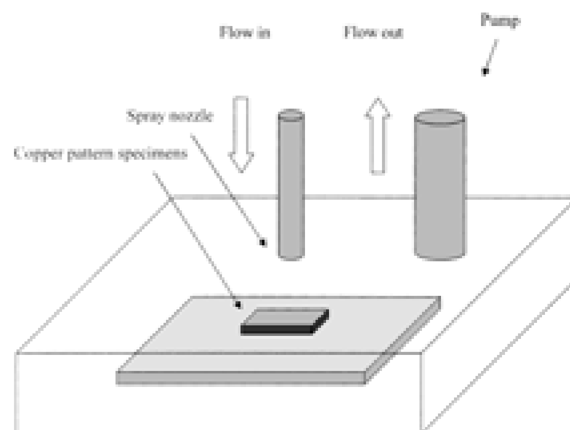

Fig. 1. Schematic diagram of the spray system for copper etching.

2.3. *Etching of copper pattern specimens*

The line/space (L/S) of copper pattern specimens used in this study was 75 μm/75 μm. Figure 1 shows the design of etching system used. The system included a pump to circulate the etchant and a spray nozzle. Each specimen was set on a holder. After etching for a specified time, the specimen was removed from the holder and washed with distilled water. Specimens were then cast in resin, cross-sectioned, mechanically polished (0.05 μm Al_2O_3) and photographed with an optical microscope.

3. Results and discussion

3.1. *Kinetics of copper dissolution*

Anodic and cathodic Tafel plots of copper electrode in various MEA-complexed cupric chloride solutions at 25 °C are shown in Figure 2. The i_{corr} at different

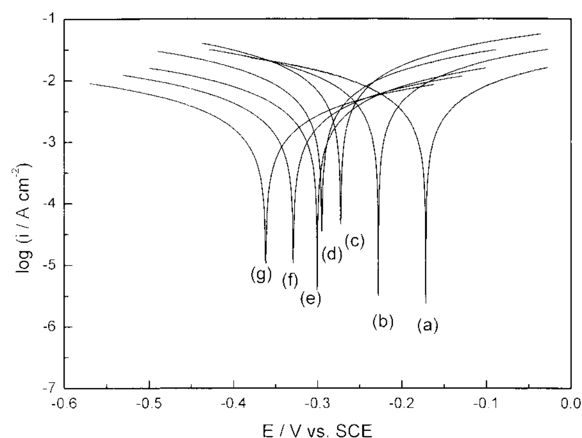

Fig. 2. Tafel plots for copper in MEA-complexed cupric chloride solution with various MEA concentrations at 25 °C: (a) 3.3, (b) 4.2, (c) 5.0, (d) 5.8, (e) 6.6, (f) 8.3 and (g) 10.0 M; [Cu(II)] = 1.0 M.

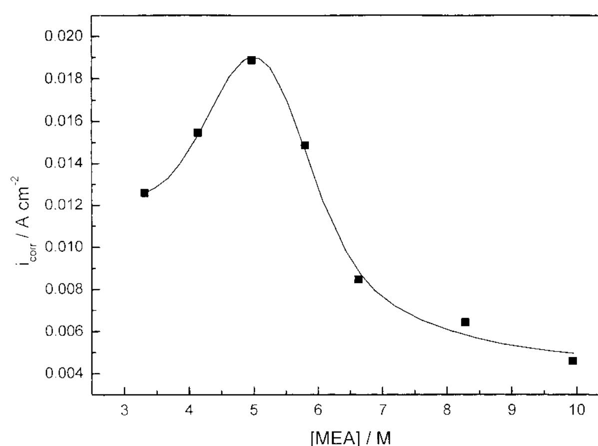

Fig. 3. Plot of corrosion current density (i_{corr}) vs MEA concentration for copper dissolution in MEA-complexed cupric chloride solutions at 25 °C; [Cu(II)] = 1.0 M.

reaction times was determined with each MEA-complexed cupric chloride solution of various MEA concentrations respectively. The values of E_{corr} and i_{corr} of copper dipped in MEA-complexed solutions are calculated by using the Tafel extrapolation method and listed in Table 1. The maximum percentage deviation was no more than 5%.

The relation between i_{corr} and the concentration of MEA is shown in Figure 3. Apparently i_{corr} increases as MEA concentration increases from 3 M to 5 M and the highest i_{corr} occurs at [MEA] around 5 M. The ratio of [MEA]/[Cu^{2+}] is about 5. However, i_{corr} decreases rapidly if [MEA] exceeds 5 M. This is probably because without sufficient MEA ligands, the formation of $[Cu^{(II)}(MEA)_4]^{2+}$ naturally slow down, so the dissolution rate decreases. The detailed reaction mechanism will be discussed later. However, excessive MEA does not help accelerate the dissolution rate, owing to the inhibitive effect of MEA ligands, as previously reported [24]. The corrosion potential was found to shift in the negative direction with increasing MEA concentration as shown in Table 1. This is the same as that found in the ammoniacal solution system [26, 27] and different from the general behaviour of inhibitor in copper corrosion systems [26, 28–31]. In addition, copper dissolution in MEA ([MEA] = 1 M) without cupric chloride being added initially has also been studied. All the measurement in this section of each sample was done at its particular reaction time. When copper is slowly dissolved in MEA, the colour of the solution changes from colourless to deep blue, as observed from u.v.–vis. spectra.

Table 1. Corrosion potential (E_{corr}) and corrosion current density (i_{corr}) of copper in various MEA-complexed cupric chloride solutions at 25 °C

MEA conc. /M	E_{corr} /mV vs SCE	i_{corr} /mA cm^2
3.3	−172	12.58
4.2	−228	15.25
5.0	−273	18.88
5.8	−288	14.85
6.6	−301	8.46
8.3	−329	6.40
10.0	−362	4.60

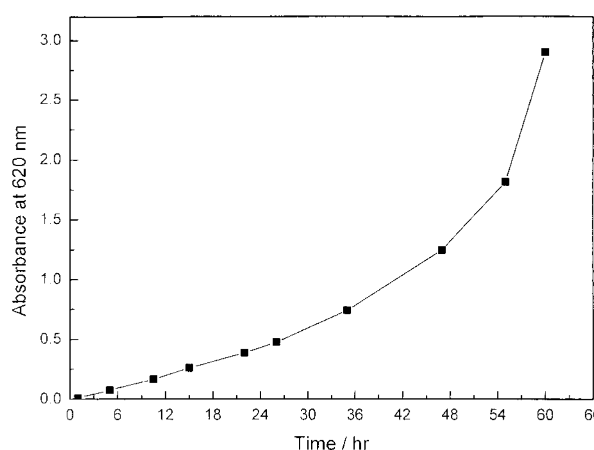

Fig. 4. Absorbance against time (h) at 620 nm, which indicates the formation of $Cu(MEA)_4^{2+}$ and its function to facilitate further copper dissolution; [MEA] = 1 M.

Figure 4 shows the absorbance of the peak at 620 nm gradually increases with time, which means the formation of $[Cu^{(II)}(MEA)_4]^{2+}$, although slow in the beginning, picks up speed when reaction continues. The response of i_{corr} and $Cu(MEA)_4^{2+}$ concentration in 1 M MEA aqueous solution is shown in Figure 5. It is apparent that the copper dissolution rate gradually increases with increasing $Cu(MEA)_4^{2+}$ concentration. This is reasonable since MEA is a chelating agent for cupric ion. Therefore, more MEA ligands help to chelate the dissolved cupric ions, which facilitate further dissolution. The rate reaches its peak when [$Cu(MEA)_4^{2+}$] about 0.2 M. At the highest i_{corr}, the ratio of [MEA]/[Cu^{2+}] is about 5, which is the same as the result shown in Figure 3. When copper was continue etched, the i_{corr} decreased. The depletion of MEA ligands leads to

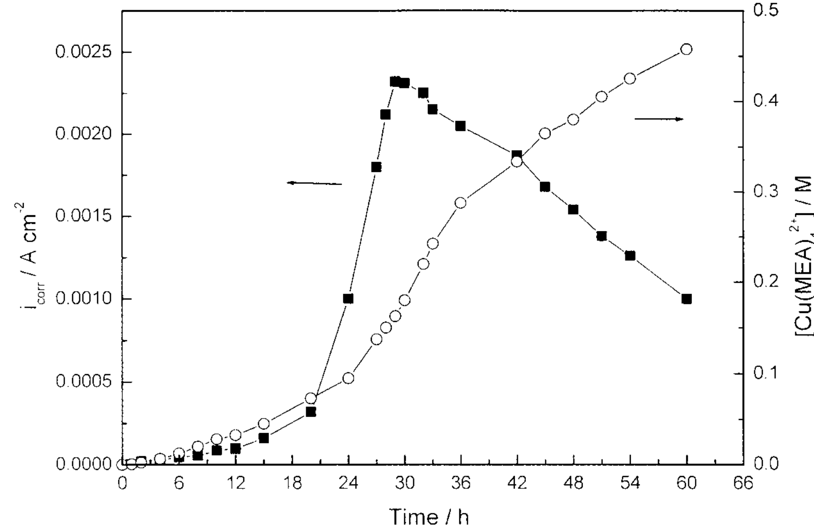

Fig. 5. i_{corr} (A cm^{-2}) and $Cu(MEA)_4^{2+}$ (M) concentration against time (h) in 1 M MEA solution. Key: (■) i_{corr} and (○) [cu(MEA)$_4^{2+}$].

insufficient concentration and the formation of $[Cu^{(II)}(MEA)_4]^{2+}$ slows down naturally.

Previous studies indicate that, air and oxygen dissolved in the etching solution greatly affect the dissolution rate [26, 33]. In ammoniacal etchant, dissolved oxygen may yield more etchant molecules [9]. In our study, the role of dissolved oxygen has also been tested. The results are shown in Figure 6. The i_{corr} of systems with air or oxygen sparging is quite stable (~0.019 A cm^{-2} for air and 0.022 A cm^{-2} for O_2). But the etching rate decays with nitrogen sparging and finally precipitation occurs, presumably insoluble cuprous oxide or salt is formed. This is because when copper is etched by $Cu(MEA)_4^{2+}$, $[Cu^{(I)}(MEA)_2]^+$ is formed as product which needs O_2 to oxidize it back to $[Cu^{(II)}(MEA)_4]^{2+}$ to continue the etching reaction. Insufficient supply of O_2 such as in the case of nitrogen sparging would lead to slowing down of the etching reaction.

The basic reaction of $[Cu^{(II)}(MEA)_4]^{2+}$ to induce copper dissolution in MEA solution containing chloride ions has been described in our previous study [24]. The chloride ion can be seen as the bridging ligand for enhancing dissolution rate. Base on the afore mentioned results, the reaction mechanism of copper dissolution in MEA-complexed cupric chloride solution proceeds smoothly according to the following reaction:

Reaction A Copper dissolution with $[Cu^{(II)}(MEA)_4Cl]^+$

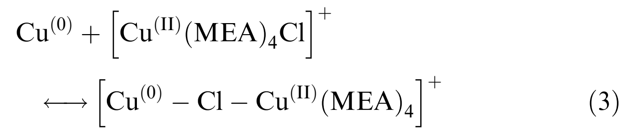

$$Cu^{(0)} + \left[Cu^{(II)}(MEA)_4Cl\right]^+ \longleftrightarrow \left[Cu^{(0)} - Cl - Cu^{(II)}(MEA)_4\right]^+ \quad (3)$$

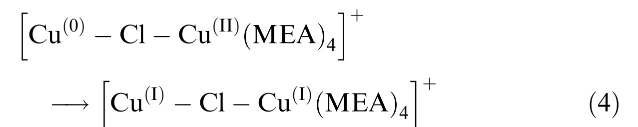

$$\left[Cu^{(0)} - Cl - Cu^{(II)}(MEA)_4\right]^+ \longrightarrow \left[Cu^{(I)} - Cl - Cu^{(I)}(MEA)_4\right]^+ \quad (4)$$

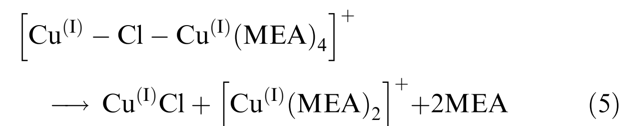

$$\left[Cu^{(I)} - Cl - Cu^{(I)}(MEA)_4\right]^+ \longrightarrow Cu^{(I)}Cl + \left[Cu^{(I)}(MEA)_2\right]^+ + 2MEA \quad (5)$$

Reaction B Regeneration of cupric complexes

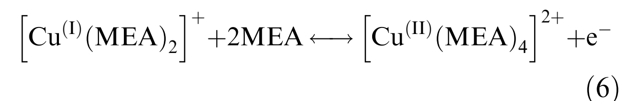

$$\left[Cu^{(I)}(MEA)_2\right]^+ + 2MEA \longleftrightarrow \left[Cu^{(II)}(MEA)_4\right]^{2+} + e^- \quad (6)$$

$$H_2O + 2O_2 + 4e^- \longleftrightarrow 4OH^- \quad (7)$$

The effect of temperature on the dissolution of copper has also been studied. The dissolution rate generally responds to temperature change according to the Arrhenius-type equation [32] as shown in Equation 8,

$$i_{corr} = A \exp\left(\frac{-E_a}{RT}\right) \quad (8)$$

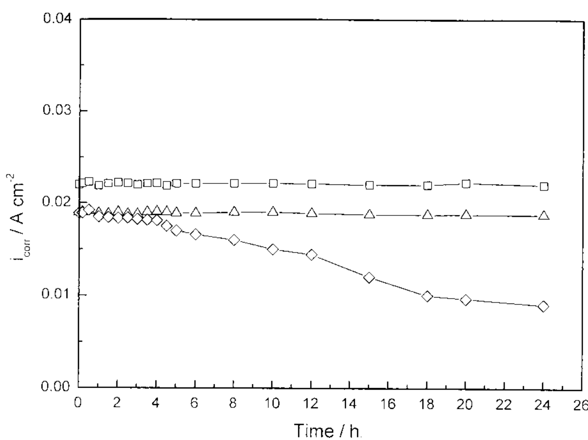

Fig. 6. The effect of oxygen, air and nitrogen sparging in MEA-complexed cupric chloride solution; [Cu(II)] = 1.0 M, [MEA] = 5 M. Key: (□) O_2, (△) air and (◇) N_2.

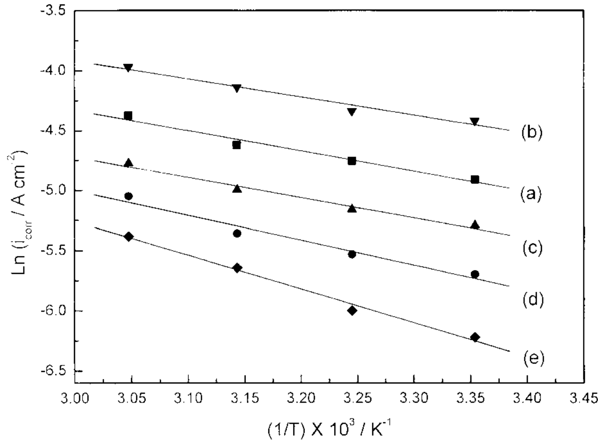

Fig. 7. Arrhenius plot showing corrosion current density against $1/T$ for copper in MEA-complexed cupric chloride solutions with different MEA concentrations; (a) 3.3, (b) 5.0, (c) 6.6, (d) 8.3 and (e) 10.0 M; [Cu(II)] = 1.0 M.

Figure 7 shows the Arrhenius plot of i_{corr} against $1/T$ for various MEA-complexed cupric solutions. The E_a value of each etchant was calculated and these values are shown in Table 2. The lowest E_a (12.53 kJ mol^{-1}) was found in solution containing 5 M MEA. Apparently, the change in E_a follows the same pattern as the change in i_{corr} in response to MEA concentration. Since E_a stands for the energy barrier for copper dissolution, excessive MEA naturally results in a greater inhibitive effect and larger E_a. However, too low a concentration of MEA leads to insufficient chelating, which also causes additional resistance to copper dissolution. Another important parameter to evaluate the etching ability of a certain ligand is the heat of adsorption (ΔH_{ads}). Many studies [28, 29, 33–35] propose that ΔH_{ads} is a good measure of the strength of adsorption on a surface. Thus, high ΔH_{ads} reflects a strong chemisorption of the ligand on the surface, and ΔH_{ads} is related to E_a as follows:

$$E_a = \Delta H_{ads} - RT \quad (9)$$

ΔH_{ads} for different MEA-complexed cupric etchants at 55 °C were calculated and are also listed in Table 2. The heat of adsorption decreases from 16.86 to 15.26 kJ mol^{-1} for MEA concentration ranging from 3.3 to 5 M and increases from 15.26 to 26.0 kJ mol^{-1} for MEA concentration ranging from 5 to 10 M. The results indicate that a strong inhibitive effect by MEA ligands occurs at high MEA concentration. Griffith and Marsh [36] found that nitrogen-containing ligands could inhibit the active sites of a copper surface, owing to the presence of lone pair electrons on the nitrogen atoms of MEA ligands. Our results support their finding.

Table 2. Activation energy (E_a) and heat of adsorption (ΔH_{ads}) for copper dissolution in various MEA-complexed cupric chloride solutions

[MEA] /M	E_a /kJ mol^{-1}	ΔH_{ads} at 55 °C /kJ mol^{-1}
3.3	14.13	16.86
4.2	13.25	15.98
5.0	12.53	15.26
5.8	13.05	15.78
6.6	14.08	16.80
8.3	17.17	19.90
10.0	23.27	26.00

The effect of pH ranging from 6.5 to 10 on copper dissolution is shown in Figure 8. Apparently, there is an optimal range of pH for effective etching of copper. As the pH is lowered from 10, the dissolution rate (i_{corr}) increases until the pH reaches about 8–7.5. The result is similar to that for copper in ammoniacal etchant [37]. Ammonia reacts with acid to produce ammonium ion ($NH_3 + H^+ \rightarrow NH_4^+$) instead of complexing with cuprous ion. This is why ammoniacal etchant etches faster in more alkaline solution. Similarly, the amine group ($-NH_2$) of MEA tends to react with acid to form an ammonium group ($-NH_3^+$), as follows:

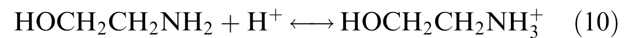

$$HOCH_2CH_2NH_2 + H^+ \longleftrightarrow HOCH_2CH_2NH_3^+ \quad (10)$$

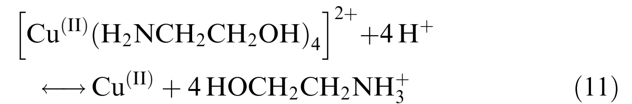

$$\left[Cu^{(II)}(H_2NCH_2CH_2OH)_4\right]^{2+} + 4\,H^+ \longleftrightarrow Cu^{(II)} + 4\,HOCH_2CH_2NH_3^+ \quad (11)$$

This naturally reduces the chance for MEA to chelate Cu^{2+} to induce copper dissolution as shown in Equations 3–5. When the pH is lower than 8–7.5, the etching rate begins to decrease rather than increase. The solution becomes unstable and the formation of a precipitate starts. This may be due to the decomposition of $[Cu^{(II)}(MEA)_4]^{2+}$, giving insufficient MEA to complex with the cuprous ions, which results in the precipitate of Cu_2O or CuCl. Thus, there is an optimal range of pH for MEA-complexed cupric solution to work as copper etchant.

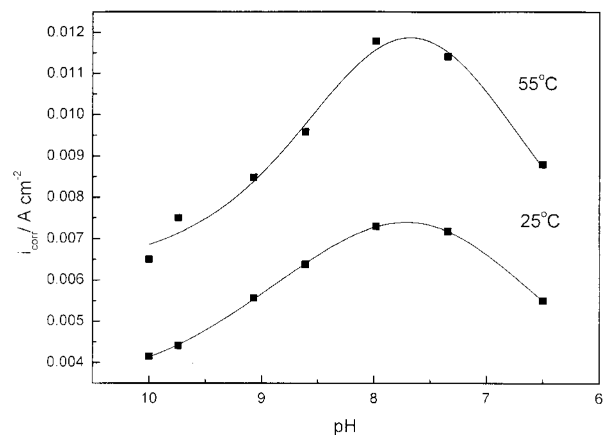

Fig. 8. Plot of corrosion current density (i_{corr}) against pH values of MEA-complexed cupric chloride solutions at 25 °C and 55 °C; [Cu(II)] = 1.0 M, [MEA] = 5.0 M.

3.2. *Etching of copper pattern*

Etching of a PCB specimen with copper pattern (75 μm/75 μm, L/S) was conducted in an etchant (1 M $CuCl_2$ and 3.3 to 10 M MEA) controlled at 55 °C and with air sparging. The maximum percentage deviation of the analysis of etching rate and etching factor was no more than 6%.

The etching results are shown in Figure 9 which exhibits the same relation as that between i_{corr} and MEA concentration (Figure 3). Copper etching in ammoniacal etchant was also measured for comparison. The etching rate is around 40~45 μm min^{-1} at 55 °C, which is faster than for the MEA system by about an order of magnitude. However, the effect of undercut after etching is also important for a certain etchant. Therefore, the etching factor of MEA-complexed cupric etchant was studied.

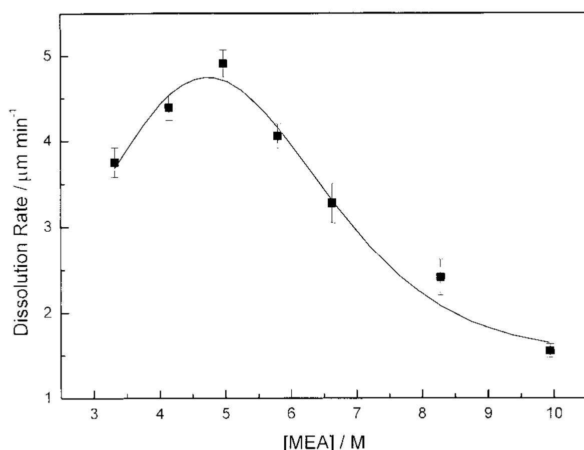

Fig. 9. Copper etching rate of different MEA-complexed cupric chloride etchants by spray method at 55 °C.

Figure 10 shows the cross section of copper foil being etched with respect to time. The copper foil was partially covered with tin resistant on top and etching started when the exposed copper contacted the etchant sprayed on it. Etching was stopped when the etched line reached the bottom substrate and approached the specified line width (75 μm). The etching factor was then calculated and served as an index of performance. Case D in Figure 10 shows the best etching effect based on etching factor. A quantitative evaluation is shown in Table 3. Obviously, the MEA-complexed cupric etchant performs much better than the ammoniacal etchant and can be considered an effective banking agent.

The effect of pH on etching of a copper pattern was also studied and results are shown in Figure 11. Again it exhibits the same relation as that between the i_{corr} and pH for MEA-complexed cupric etchants (Figure 8). This means that the etching process under spray conditions is totally controlled by electrochemical kinetics. The highest etching rate can reach about 9 μm min^{-1} at pH around 7.7, which is about twice as

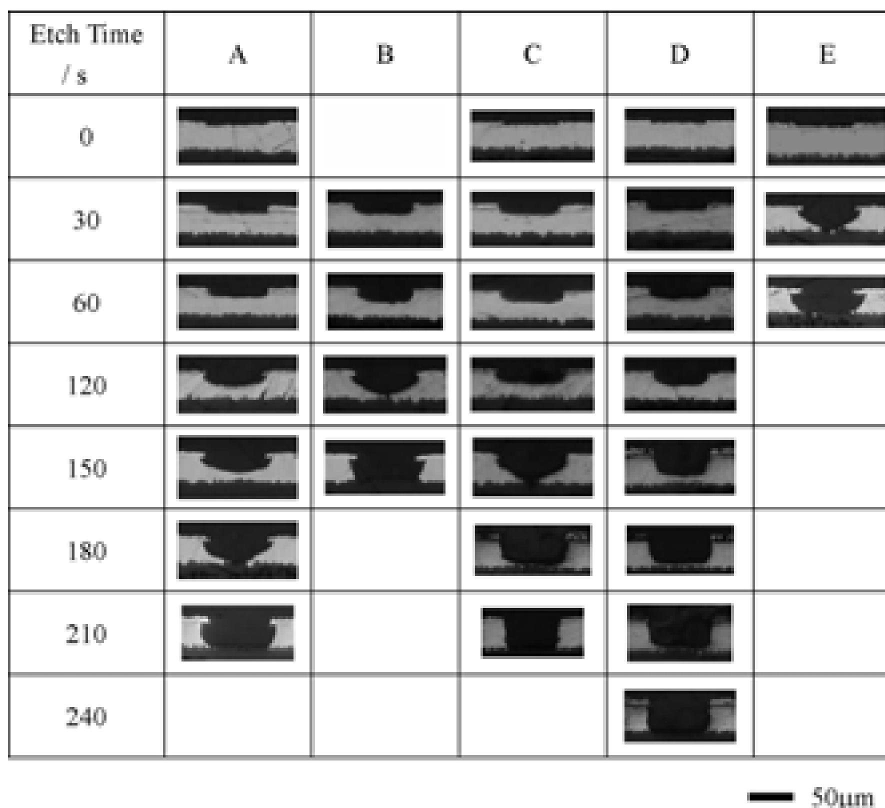

Fig. 10. Etching progress of PCB sample of 34 μm thick copper foil with a 75 μm/75 μm (L/S) solder resist, MEA-concentrations: (A) 3.3, (B) 5.0, (C) 6.6 and (D) 10.0 M, (E) commercial ammoniacal etchant for comparison.

Table 3. Etching factors of 75 μm/75 μm (L/S) copper pattern specimens in MEA-complexed cupric etchant of different MEA concentrations: (A) 3.3, (B) 5.0, (C) 6.6 and (D) 10.0 M, and (E) commercial ammoniacal etchant for comparison

Sample	[MEA]/M	Etching factor
A	3.3	3.31 ± 0.20
B	5.0	4.12 ± 0.12
C	6.6	5.06 ± 0.25
D	10.0	5.23 ± 0.25
E	–	1.88 ± 0.18

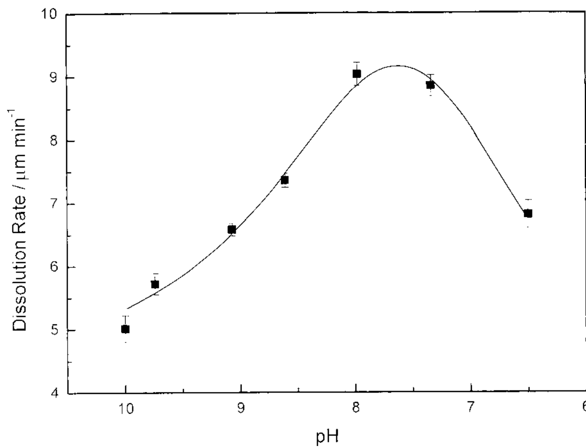

Fig. 11. Copper etching rate in MEA-complexed cupric chloride etchant at various pH values by spray method at 55 °C; [Cu(II)] = 1.0 M, [MEA] = 5.0 M.

high as that at pH greater than 10. So the etching rate is not only influenced by the concentration of MEA, as shown in Figure 3, but also by the etchant pH. Figure 12 shows the etching behaviour of copper foil (thickness 34 μm) with a 75 μm/75 μm (L/S) tin resist. The etching factor of these four systems was calculated

Table 4. Etching factors of 75 μm/75 μm (L/S) copper pattern specimens in MEA-complexed cupric chloride etchant at various pH values; [Cu(II)] = 1.0 M, [MEA] = 5.0 M

pH	Etching factor
10.00	4.12 ± 0.12
9.07	3.33 ± 0.34
7.98	2.67 ± 0.35
7.34	2.22 ± 0.25

and results are listed in Table 4. It is obvious that the foil suffers more undercut as pH is decreased. Since MEA serves as a banking agent, the addition of acid consumes MEA, which consequently results in more severe undercut. Thus, an optimal etching condition can be decided as a compromise between etching and etching factor.

4. Conclusions

MEA-complexed cupric ion solution is a promising etchant. It is also a superior banking agent because of its inhibitive property. This etchant shows an optimal composition regarding the MEA concentration and pH. The optimal MEA concentration is around 5 M for 1 M $CuCl_2$ and the optimal pH is around $8 \sim 7.5$ based on etching rate.

The etching factor is also influenced by the MEA concentration and pH. It increases from 3.31 to 5.23 as the MEA concentration increases from 3.3 to 10.0 M and it decreases from 4.12 to 2.22 as the pH of the etchant decreases from 10 to 7.34. Further, the etching factor of MEA-complexed etchant can be much higher than the commercial ammoniacal etchant. However, the latter produces much faster etching.

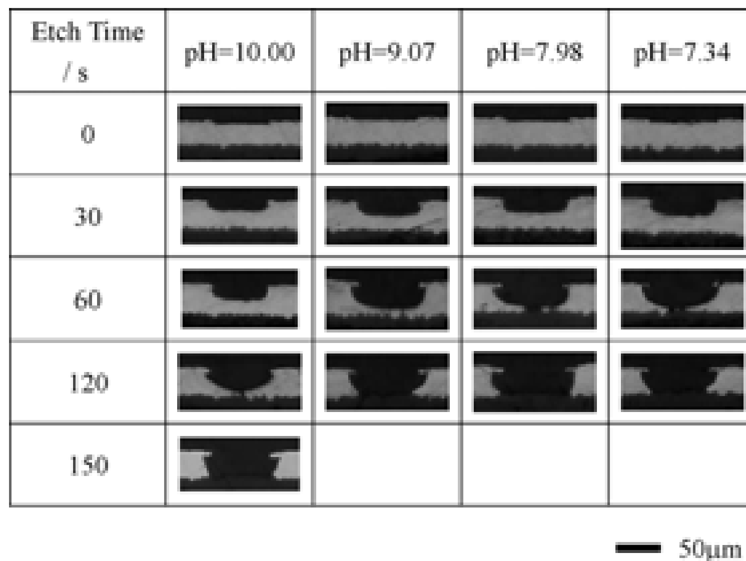

Fig. 12. Etching progress of PCB sample of 34 μm thick copper foil with a 75 μm/75 μm (L/S) solder resist.

References

1. R.E. Morris, *Electroplat. Metal Finish*. Feb. (1972).
2. C.F. Coombs Jr, 'Printed Circuits Handbook' (1988), chapter 14.
3. K.L. Covert and J.A. Kurowski, *J. Electrochem. Soc*. **139** (1992) 2202.
4. R.W. Lay, *Electronic Packaging and Production*, March, (1982), p. 65.
5. H. Markstein, *Electronic Packaging and Production*, Feb. (1985), p. 65.
6. L.H. Tseng, MS thesis, Tsing-Hua University Taiwan (June, 1998).
7. C.W. Lin, M.S. Thesis, Tsing-Hua University, Taiwan (June, 1999).
8. D.J. Sykes, *US Patent 4 311 551* (1982).
9. R.H.W. Richardson and C.F. Jordan, *US Patent 5 431 776* (1995).
10. R. Alkire and H. Deligianni, *J. Electrochem. Soc*. **133** (1988) 1093.
11. C.B Shin and D.J. Economou, *J. Electrochem. Soc*. **136** (1989) 1997.
12. D. Papapanayiotou, H. Deligianni and R.C. Alkire, *J. Electrochem. Soc*. **145** (1998) 3016.
13. M. Georgiadou and R.C. Alkire, *J. Electrochem. Soc*. **140** (1993) 1340.
14. T. Yamamoto, T. Kataoka and J. Andresakis. *Circuit World* **27** (2000) 6.
15. P. Borth and P. Forest, *US Patent 3 514 409* (1970).
16. K.J. Murski, *US Patent 4 319 955* (1982).
17. D. Papapanayiotou, H. Deligianni and R.C. Alkire, *J. Electrochem. Soc*. **145** (1998) 3016.
18. N.I. Sax, 'Dangerous Properties of Industrial Materials' (Reinhold, New York, 1957), p. 464.
19. C.R. Shipley Jr, *US Patent 3 650 958* (1972).
20. R.J. Flannery, B. Ke, M.W. Grieb and D. Trivich, *J. Am. Chem. Soc*. **77** (1955) 2996.
21. C.C. Nathan, '*Corrosion Inhibitors*' (NACE, Houston, TX, 1973).
22. X.Q. Wang and Y.F. Zhang, *Key Eng. Mater*. **20** (1987) 2799.
23. A. El-Sayed, F. Rashwan and F. El-Cheikh, *Mater. Chem. Phys*. **46** (1996) 61.
24. C.C. Shih, Y.Y. Wang and C.C. Wan, *J. Appl. Electrochem*. (2002), submitted.
25. R. Gašparac and E. Stupnišek-Lisac, *Corrosion* **55** (1999) 1031.
26. Q. Luo, R.A. Mackay and S.V. Babu, *Chem. Mater*. **9** (1997) 2101.
27. A. Darchen and R. Drissi-Daoudi, *J. Appl. Electrochem*. **27** (1997) 448.
28. G.K. Gomma, *Mater. Chem. Phys*. **55** (1998) 131.
29. G.K. Gomma, *Mater. Chem. Phys*. **56** (1998) 27.
30. V.B. Singh and R.N. Singh, *Corros. Sci*. **37** (1995) 1399.
31. S. Sankarapapavinasam and M.F. Ahmed, *J. Appl. Electrochem*. 22 (1992) 390.
32. R. Gašparac, C.R. Martin and E. Stupnišek-Lisac, *J. Electrochem. Soc*. **147** (2000) 548.
33 S. Sankarapapavinasam, F. Pushpanaden and M.F. Ahmed, *Corros. Sci*. **32** (1991) 193.
34. B.H. Loo, A. Ibrahim and M.T. Emerson, *Chem. Phys. Lett*. **287** (1998) 449.
35. R. Babic, M. Metikos-Hukovic and M. Loncar, *Electrochim. Acta* **44** (1999) 2413.
36. R.H. Griffith and J.D.F. Marsh, '*Contact Catalysis*' (Oxford University Press, Oxford, 1957), p. 193.
37. M.W. Jawitz, '*Printed Circuits Materials Handbook*' (1997), chapter 15.